# Imaging multiphoton ionization dynamics of $CH_3I$ at a high repetition rate XUV free-electron laser



OPEN ACCESS
IOP Publishing
Journal of Physics B: Atomic, Molecular and Optical Physics
J. Phys. B: At. Mol. Opt. Phys. **54** (2021) 014001 (9pp)
https://doi.org/10.1088/1361-6455/abc6bc

# Imaging multiphoton ionization dynamics of $CH_3I$ at a high repetition rate XUV free-electron laser

**Yu-Chen Cheng[1], Bart Oostenrijk[1], Jan Lahl[1], Sylvain Maclot[1,2], Sven Augustin[3,4,5], Georg Schmid[3], Kirsten Schnorr[3,5], Severin Meister[3], Dimitrios Rompotis[6,7], Bastian Manschwetus[6], Harald Redlin[6], Cédric Bomme[6], Benjamin Erk[6], Daniel Rolles[4,6], Rebecca Boll[6,7], Pavel Olshin[8], Artem Rudenko[4], Michael Meyer[7], Per Johnsson[1], Robert Moshammer[3] and Mathieu Gisselbrecht[1,*]**

[1] Department of Physics, Lund University, P.O. Box 118, 22100 Lund, Sweden
[2] Department of Physics, University of Gothenburg, Origovägen 6B, 41296 Gothenburg, Sweden
[3] Max-Planck-Institut für Kernphysik, D-69117 Heidelberg, Germany
[4] J R Macdonald Laboratory, Department of Physics, Kansas State University, Manhattan, KS 66506, United States of America
[5] Paul Scherrer Institut, Forschungsstrasse 111, 5232 Villigen, Schweiz
[6] Deutsches Elektronen-Synchrotron (DESY), D-22607 Hamburg, Germany
[7] European XFEL GmbH, D-22869 Schenefeld, Germany
[8] Saint-Petersburg State University, 199034 St. Peterburg, Russia

E-mail: mathieu.gisselbrecht@sljus.lu.se

Received 1 September 2020
Accepted for publication 2 November 2020
Published 18 December 2020

**Abstract**

XUV multiphoton ionization of molecules is commonly used in free-electron laser experiments to study charge transfer dynamics. However, molecular dissociation and electron dynamics, such as multiple photon absorption, Auger decay, and charge transfer, often happen on competing time scales, and the contributions of individual processes can be difficult to unravel. We experimentally investigate the Coulomb explosion dynamics of methyl iodide upon core–hole ionization of the shallow inner-shell of iodine (4d) and classically simulate the fragmentation by phenomenologically introducing ionization dynamics and charge transfer. Under our experimental conditions with medium fluence and relatively long XUV pulses (∼75 fs), we find that fast Auger decay prior to charge transfer significantly contributes to the charging mechanism, leading to a yield enhancement of higher carbon charge states upon molecular dissociation. Furthermore, we argue for the existence of another charging mechanism for the weak fragmentation channels leading to triply charged carbon atoms. This study shows that classical simulations can be a useful tool to guide the quantum mechanical description of the femtosecond dynamics upon multiphoton absorption in molecular systems.

Keywords: recoil-ion momentum spectroscopy, methyl iodide dissociation, sequential ionization, charge transfer, Auger decay

(Some figures may appear in colour only in the online journal)

* Author to whom any correspondence should be addressed.

## 1. Introduction

Free-electron-lasers (FELs) [1–4] have opened new avenues to investigate ultrafast dynamics with short wavelength photons using non-linear light–matter interaction processes [5, 6]. Following multiple photon absorptions, highly charged molecular systems undergo Coulomb explosion [7] allowing for monitoring the real-time dynamics of molecules as they break apart [8–11], as well as charge transfer between constituent atoms [6, 12–14]. However, ionization, Auger decays and charge transfer can occur on competing time scales, often hampering the possibility to uncover the details of individual processes. Detailed descriptions of charge dynamics are needed to understand the fragmentation process, but they represent a great theoretical challenge due to a large number of parameters, some of which might be poorly known [6, 15]. Simplified models, such as the generalised two-parameter model introduced by Motomura *et al* [16] to describe the charge buildup and the charge transfer processes, may provide satisfactory agreement with experiments, but can only provide a qualitative understanding. Computationally efficient simulations should therefore be further developed.

Organohalides have been used in the recent years as model systems to investigate the interplay between ultrafast electron and nuclear dynamics [6, 12, 14, 16]. Due to the high absorption cross section of halogen atoms above many of their inner-shell absorption edges, element-selective multiple inner-shell ionization allows for the initial localization of charges on one atom. A common picture has emerged from these studies, see figure 1(a). As electrons are sequentially stripped away from the halide atom by photon absorptions and (multiple) Auger decays, the Coulomb repulsion forces drive the dissociation dynamics, while electron charge transfer occurs from the rest of the molecule toward the halide. The experimental results found using time-resolved pump–probe techniques involving laser photoexcitation [12, 14] allowed to validate the classical over the barrier model (COB) [17, 18] to describe the charge transfer mechanism. Details of the fragmentation dynamics can also be unraveled with multi-coincidence 3D imaging spectrometers in the multiphoton regime. These spectrometers can be used to benchmark new simulation methods but require (ideally) high repetition rate FELs to obtain sufficient statistics.

In this work, we investigate the Coulomb explosion of methyl iodide after absorption of multiple photons in the vicinity of the giant resonance of the iodine 4d-shell at 90 eV, with relatively long light pulses (∼75 fs). In contrast to previous work [9, 19], we carried out our experiment with a 3D imaging spectrometer to study the fragmentation dynamics of low charge states (⩽13 charges). We performed classical nuclear wavepacket dynamics simulations to gain deeper insight into the dynamics of fragmentation beyond the generalized two-parameters model [16]. In our simulation, the molecular charging mechanisms are driven by the ionization and normal Auger decay, which occurs sequentially between the absorption of two photons during the early ionization steps of iodine [20, 21]. The charge transfer mechanism is assumed to occur instantaneously and is primarily described by the COB model [6, 12, 14]. Using this assumption, we can successfully explain the formation of doubly charged carbon atoms but not triply charged ones. To produce such a highly charged carbon ions, we show that a more complete description of the 4d-shell ionization of highly charged iodine is essential.

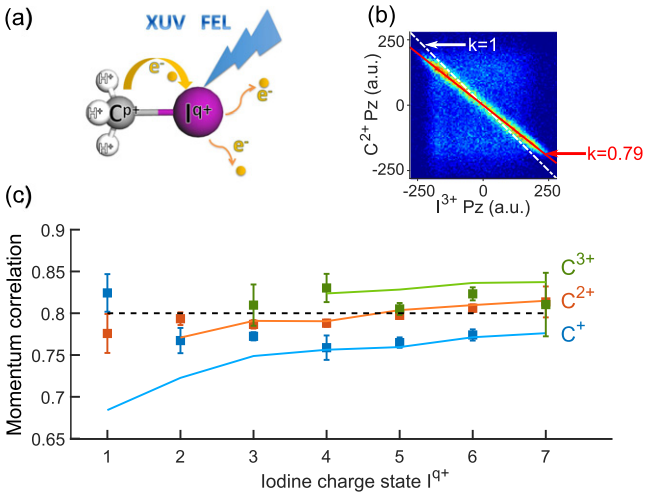


**Figure 1.** (a) Illustration of the charging and charge transfer mechanisms upon element-selective multiple inner-shell ionization of methyl iodide. (b) Momentum distribution of coincident $C^{2+}$ and $I^{3+}$ ions (in atomic units). The factor $k$ of the white dash-dotted line is 1, corresponding to a pure two-body break up (see text). (c) Momentum correlation coefficient $k$, i.e. the momentum ratio between carbon and iodine as a function of iodine charge state, for three different carbon charge states. The square points are the experimental data, and the solid lines correspond to simulated results for different carbon groups (see main text). The dashed line indicates the correlation coefficient for a sequential (two-step) breakup.

## 2. Methods

The experiment was performed at the FLASH free-electron laser at DESY in Hamburg with a reaction microscope (REMI) spectrometer installed in the CAMP chamber of the BL1 beamline [22]. The FLASH FEL was running at high repetition rate with 10 bunch trains per second, each containing 42 mini-bunches with a spacing of 10 $\mu$s, i.e. 420 pulses per second. At a photon energy of 90 eV, the XUV pulse duration was estimated to be 75 fs (55% of the electron bunch width [23]). Tight focusing of the 0.9 $\mu$J XUV pulses to a 6 × 8 $\mu$m focus spot provided an intensity up to $2.5 \times 10^{13}$ W cm$^{-2}$, which is sufficient for sequential multiphoton ionization but not enough to reach the $I^{8+}$ charge state that requires the simultaneous absorption of two photons in the last ionization step [24]. The electric field of the REMI spectrometer was set to 80 V cm$^{-1}$ to record the heaviest ion, $CH_3I^+$, within 10 $\mu$s. The total count rate was adjusted to 1–2 counts per XUV pulse by controlling the pulse energy with a gas attenuator to ensure enough statistic of the coincident spectra. The spectrometer was modeled with SIMION [25] to account for the decrease of the detection efficiency of high energetic ions, allowing us to compare the fragment pair yields with reported values recorded without the coincidence technique [19].

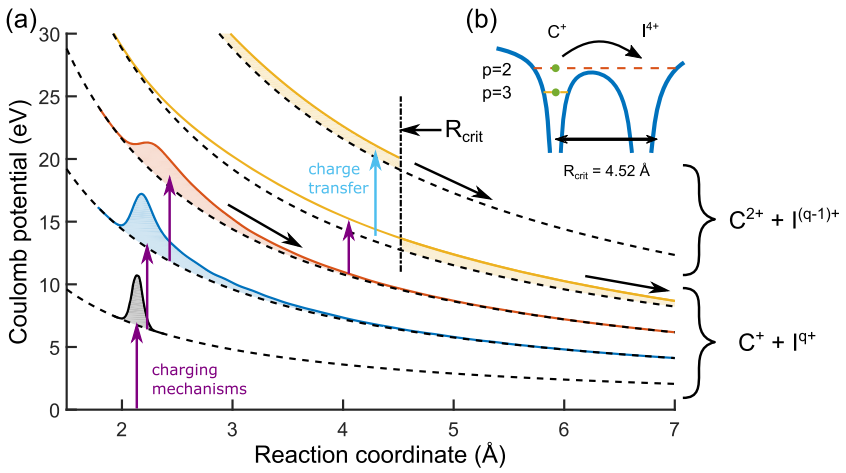


**Figure 2.** (a) Schematic time evolution of a nuclear wave packet on Coulomb potential energy curves. Purple arrows symbolize charging mechanisms due to sequential ionization or Auger decay. The blue arrow represents the charge transfer between the carbon and iodine ions depicted within the COB model. (b) Example of the COB model showing that the maximum of the classical potential energy between the two nuclei is below the atomic orbital energy as long as the carbon–iodine inter-nuclear distance is below the critical distance $R_{\mathrm{crit}}$. In this case, the charge transfer from $C^+$ to $I^{4+}$ is allowed.

For our experimental conditions, multi-photon ionization of $CH_3I^+$ occurs via sequential multiple photon absorption. Multiply charged fragment pairs up to $C^{p+}$ ($p = 3$) and $I^{q+}$ ($q = 7$) are observed, where all hydrogen atoms have been removed upon dissociation. The momenta imparted to the hydrogens can nonetheless be inferred from the fragment pair by introducing the momentum correlation coefficient, $k$, defined in a three-fold symmetry breakup as [16]:

$$\vec{p}_{C^{p+}} + k \cdot \vec{p}_{I^{q+}} = \vec{0}, \tag{1}$$

where $\vec{p}_{C^{p+}}$ and $\vec{p}_{I^{q+}}$ are the momenta of $C^{p+}$ and $I^{q+}$, respectively. Figure 1(c) shows the values of this coefficient, which is experimentally determined from the axial momentum correlation plot between two fragments, as exemplified for the $(C^{2+}, I^{3+})$ channel in figure 1(b). The values of k are around $0.8 \pm 0.04$, which is close to the mass ratio between the carbon and the methyl group (black dashed line). This suggests that the emission of hydrogen atoms has a small contribution to the kinematic of fragmentation. The fragmentation dynamics can be seen as a sequential breakup, where the bond between the methyl group and iodine breaks faster than the bonds between carbon and hydrogen atoms. Charged fragments with hydrocarbons, $CH_x$ ($x = 1, 2, 3$) are only detected in coincidence with a carbon charge state of one, in accordance with other FEL experiments [6, 16].

Using classical nuclear wavepacket dynamic simulations, we investigated the role of individual processes, such as ionization, Auger decay and charge transfer, upon fragmentation. Assuming all hydrogen atoms equivalent upon fragmentation [16], the molecule is treated with a three-fold symmetry as three point charges, and the equations of motion are solved with Coulomb potential energy curves. The charging mechanism and charge transfer are introduced phenomenologically. For charging the molecule, a random sequence in time of photoionization in iodine is generated, followed by normal Auger decay and instantaneous charge transfer to the methyl group. Note that the primary charging mechanism is supposed to be sequential photoionization [20, 21] at an iodine charge state above 3 (see appendix A for further details). Initially, the charge transfer primarily originates from the delocalization of the holes in the valence orbitals, and we introduced a fractional charge on hydrogen atoms to redistribute the charge density (that can spread over carbon and hydrogen atoms), as done previously [16]. By default, the simulations assume that all hydrogen atoms are fully charged after three-photon absorption, unless otherwise stated. As the molecular bonds elongate, the iodine can continue to charge up, and the carbon atom can continue contributing to charge transfer [6, 12, 14]. The charge transfer mechanism between atoms is introduced using the COB model [17, 18].

The carbon–iodine elongation is described by a nuclear wavepacket starting from an initial neutral molecular geometry. The principle of nuclear wavepacket dynamics is presented in figure 2 (a) for three-photon absorption. Charging mechanisms project the nuclear wavepacket to a Coulomb potential energy curve correlated to a dissociation limit $(C^+, I^{q+})$, resulting in a higher final charge state of iodine. This dissociation limit is related to the fragment pair measured in the experiment. As long as the inter-nuclear distance between atoms is smaller than a critical distance, $R_{\mathrm{crit}}$, electrons from the outermost occupied shell can migrate from one site to another provided that it is energetically favorable [24], see figure 2(b). In the case of ($p$) charges on carbon atoms and ($q$) charges on iodine, the critical distance can be expressed as:

$$R_{\mathrm{crit}} = \frac{(p+1) + 2\sqrt{(p+1)q}}{I_p}, \tag{2}$$

where $I_p$ is the binding energy of the outermost shell in the $C^{p+}$ ion. For a measured fragment pair $(C^{2(3)+}, I^{q+})$, the charge transfer may happen for different charge state of iodine. We denoted as pathway, CT$pq$, the charge transfer occurring when iodine accumulates $q$ charges in a $C^{p+}$ channel leading to the

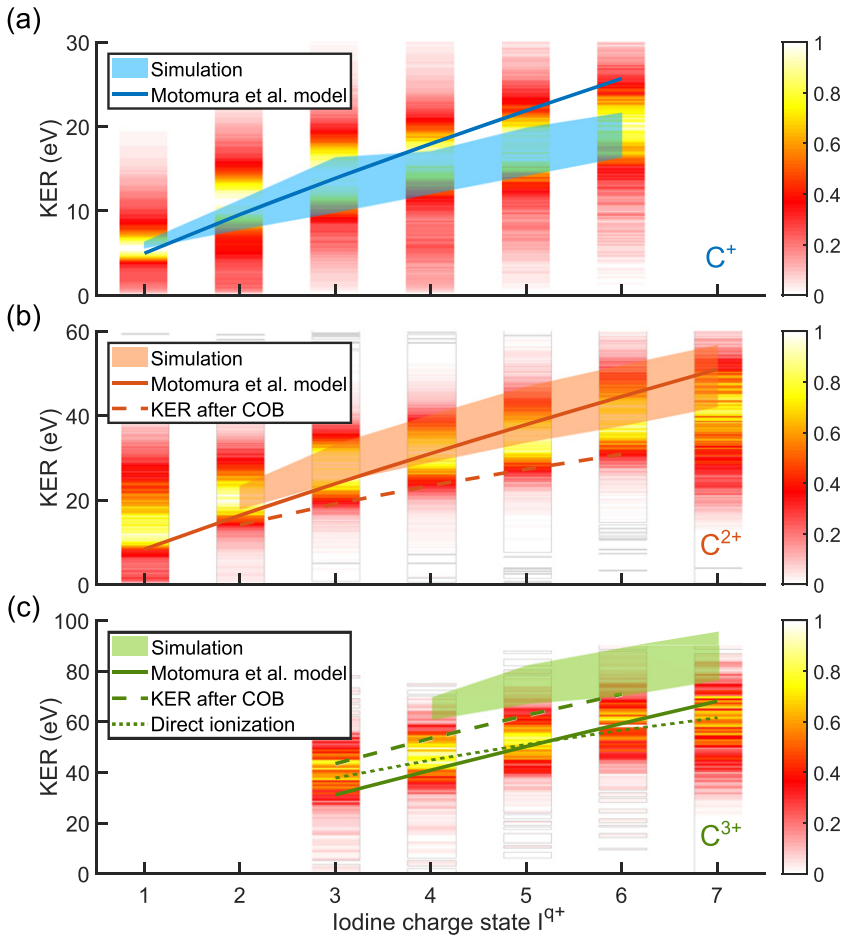


**Figure 3.** KER of carbon–iodine ion pairs as a function of the iodine charge state for (a) $C^+$, (b) $C^{2+}$ and (c) $C^{3+}$. Experimental data are shown with normalized heat map color, Monte-Carlo simulations in shaded areas, and the results from Motomura's model with solid lines. In (b) and (c), the dashed lines correspond to the KER after charge transfer at the critical distance, $R_{crit}$. In (c), the dotted-line indicates the KER obtained directly after ionization of $C^{2+}$ charge states without nuclear dynamics.

formation of $C^{p+1}$. The CT14 pathway is illustrated in figure 2 (a). The nuclear wave packet below the critical distance, $R_{crit}$, is transferred to Coulomb potential energy surfaces with $C^{2+}$ charge state, while the remaining nuclear wave packet above $R_{crit}$ keeps moving along the lower potential energy surfaces correlated to dissociation limits with a $C^+$ charge state.

Using Monte-Carlo methods, all physical quantities such as the momentum correlation coefficient, kinetic energy release (KER), and branching ratios between fragmentation channels ($C^{p+}$, $I^{q+}$) are determined. Finally for comparison, we also applied the Motomura model based on two parameters [16]. The best parameters that reproduced the measured KER are a charge build-up time $\tau = 35$ fs and a charge transfer rate $R = 0.25$ fs$^{-1}$.

## 3. Results

We present in figures 3(a)–(c) the KER of the dissociation into carbon $C^+$, $C^{2+}$ and $C^{3+}$ detected in coincidence with $I^{q+}$ ($q = 1, \ldots, 7$), as a heat map. Our simulations are displayed as shaded areas, and the results of Motomura's model [16] with solid lines. The general behavior is very well reproduced by both models, and the KERs of all pairs increase as a function of the iodine charge state, as expected from a dissociation driven by Coulomb repulsion. In our simulation, the thickness of the shaded areas represents the upper and lower limits of the KERs obtained from the different pathways that contribute to the charge transfer (within a standard deviation of the simulated distributions). The shaded areas overlap with the maxima of the broad experimental KER distribution for the $C^+$ and $C^{2+}$ channels (white/yellow colors). The broad distribution in KER originates primarily from the nuclear wavepacket dynamics on the Coulomb energy surface. The nuclear wavepacket is strongly dispersed already after the formation of a few charges (e.g. see figure 2). Surprisingly, the KER for $C^{3+}$ is overestimated.

To understand the underlying reason of this difference, we indicate in figures 3(b) and (c) the KER calculated at the critical distance defined by the COB model, i.e. the charge transfer occurring at the longest internuclear distance, with dashed lines. For the production of $C^{2+}$, the dashed line lies on the lower side of the experimental KER distribution, indicating that the charge transfer for $C^{2+}$ channels can be described by the COB model. The good agreement between our observation and the simulations for both $C^+$ and $C^{2+}$ channels confirm the validity of this model, in agreement with the findings reported

by Braußе *et al* [9]. Now turning to the charge transfer leading to the production of $C^{3+}$ (figure 3(c)), the KER predicted by the COB model is already higher than the average of the measured distribution, explaining why our simulations can only overestimate the KER. We can thus conclude that an additional mechanism must lead to the production of $C^{3+}$.

In contrast to our simulation, the Motomura model is seemingly performing better for the $C^{3+}$ channels but only provides a mean value of the KER that is under (over) estimated at low (high) charge states of iodine, respectively. However, a deeper analysis of the time evolution of the charging mechanisms also points out some limitations of this model (see appendix A). The overall charging dynamic can extend over a long time scale, when the FEL intensity is very weak, and an artificial delayed charge built-up time of iodine acts as a 'knob' adjusting the KER to the experimental results.

The relative yields of multiply charged carbon and iodine ions are shown in figure 4(a) at two FEL pulse energies: 0.4 $\mu$J and 0.9 $\mu$J, in dashed and solid lines respectively. These ionization yields decrease for the highest iodine charge state, as expected for multiphoton processes in a perturbative regime. By integrating events over all iodine charge states at 0.9 $\mu$J, we found that the measured branching ratios of $C^{p+}$ states are in very good agreement with reported values, ranging from 79%, 20%, to 1% for $p = 1$, 2 and 3, respectively [19]. For the lower charge states of iodine, $q \leqslant 3$, the yields of a given carbon state are almost identical for the two FEL pulse energies, suggesting that channels leading to the formation of multiply charged carbon are open as soon as the molecule absorbs a few photons. To explain these yields, the experimental and simulated ratios of $(C^{p+}, I^{q+})/(C^{(p-1)+}, I^{(q+1)+})$ are investigated. In the following, we quantify for a given iodine charge state the individual contributions of the charge transfer pathways CT1$q$ and CT2$q$, leading to the formation of $C^{2+}$ and $C^{3+}$, respectively.

In figure 4(b), we present results related to the formation of the $C^{2+}$. A remarkable agreement between the experimental (wide bar charts) and the simulated (narrow bar charts) ratios is found for both charge transfer pathways CT13 and CT14, implying that these pathways primarily contribute to our observations. The simulated ratios for high charge states of iodine are much smaller, suggesting that charge transfer for high charge states of iodine is unlikely. The simulation allows us to conclude that once a charge transfer has occurred, the contribution of all other charge transfer pathways accounts for at most a few percent, and can thus be neglected. We can therefore infer that charge transfer occurs at small internuclear distances, typically $<4 \sim 5$ Å between carbon and iodine atoms. Finally, this analysis points out that the relative fragment yields of $C^{2+}$–$I^{(q-1)+}$ is relatively independent on the FEL pulse energy, as observed in our experimental conditions, because the charge transfer occurs for the lowest charged states of iodine. Note that the differences observed for the $(C^{2+}, I^{1+})$ channel can stem from the limited validity of the Coulomb explosion model at very low charge states of the molecule. In this case, ultrafast molecular motion/nuclear rearrangement may occur, resulting in a non three-fold symmetry break-up as discussed by Erk *et al* [26]

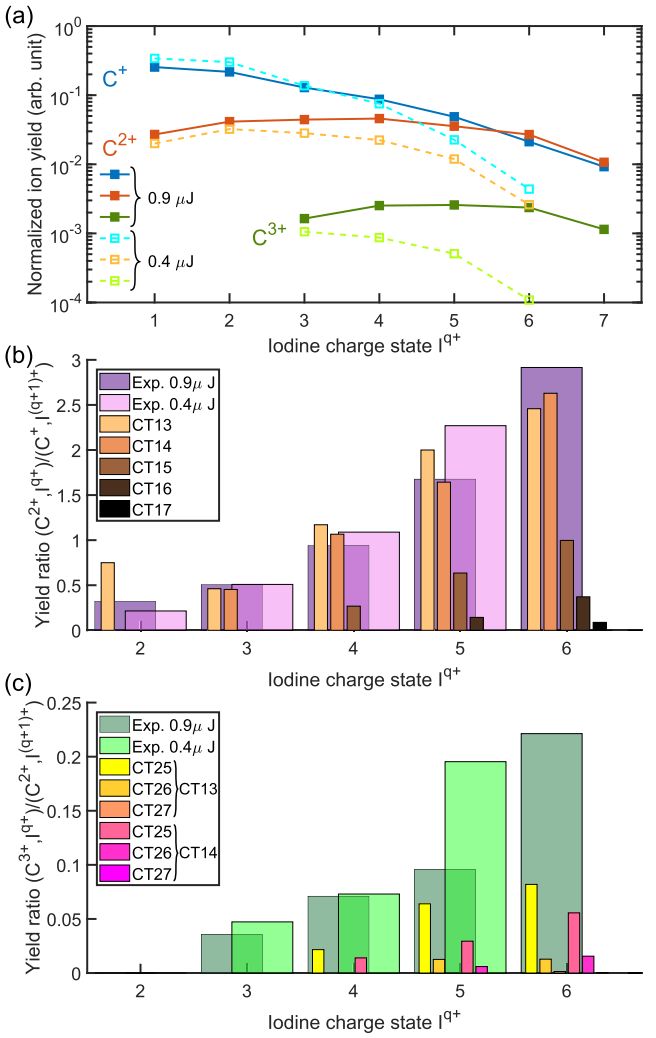


**Figure 4.** Branching ratios represented in two different ways: (a) The normalized ion yield of each carbon-iodine charge state with two experimental conditions: 0.9 and 0.4 $\mu$J. (b) The ratio $(C^{2+}, I^{q+})/(C^{+}, I^{(q+1)+})$ as a function of iodine charge state $I^{q+}$. The experimental ratios are shown with the widest bars for two different pulse energies. The $(C^{+}, I^{7+})$ charge state is not detected under the 0.4 $\mu$J condition. The narrowest bars are the simulated contributions from different charge transfer pathways CT1q, occurring from the initial $C^{+}$–$I^{q+}$ to $C^{2+}$–$I^{(q-1)+}$. Similarly, in (c) the ratio $(C^{3+}, I^{q+})/(C^{2+}, I^{(q+1)+})$ is presented as a function of iodine charge state $I^{q+}$.

While our classical simulations based on the COB model successfully reproduce the yields of formation of the $C^{2+}$ channels, they can only explain in average ~35% of the production of $C^{3+}$, see figure 4(c). As discussed previously, the formation of $C^{3+}$ would require that two charge transfers occur at small internuclear distances, resulting in a too high KER. Following the COB model, such a double charge transfer can only happen before the nuclear wavepacket has reached its critical distance. The charging mechanism should be fast and therefore, we found that the lifetime of the Auger decay is an important factor. The best agreement for the yields of both $C^{2+}$ and $C^{3+}$ was achieved for an Auger lifetime of ~2 fs, similar to the value of the neutral atomic iodine [27].

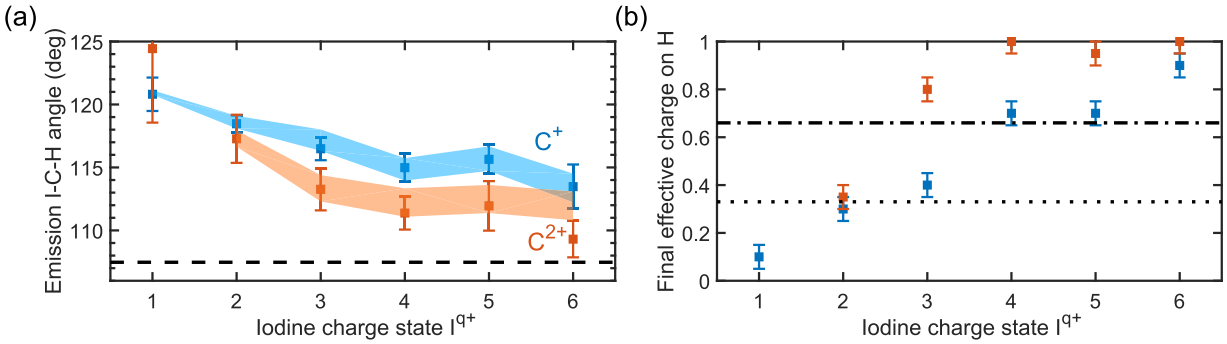


**Figure 5.** Hydrogen related dynamics in the methyl group for $C^+$ (blue) and $C^{2+}$ (red) channels. (a) Hydrogen emission angle with respect to the axis given by ($C^{p+}$–$I^{q+}$). The error bars represent the experimental uncertainties of the angles, shaded areas represent the results of the simulation, and the dashed lines indicate the angle for the neutral molecule at equilibrium. (b) Simulated final effective charge on hydrogen in the methyl group. The dotted and dashed-dotted lines show the effective number of charged hydrogens (i.e. 1, 2 hydrogens).

## 4. Discussion

The increased production of $C^{3+}$ ions in the experiment as compared to our simulations reveals that part of the electron dynamics is not properly taken into account by the simulations. From a quantum mechanical perspective, mainly two aspects should be considered: the ionization dynamics in the 4d-shell for highly charged ions, and the charge delocalization and transfer of the methyl group itself.

Upon iodine 4d-shell ionization, it is expected in analogy to multiply charged xenon [28, 29] that a transfer of the 4d oscillator strength occurs from the continuum part to the discrete part of the cross section in iodine. Hence, as the shape resonance for the charge states above $I^{3+}$ vanishes [20, 21], the initially (iodine) localized ionization may be less element specific when iodine is highly charged. The carbon/iodine ionization cross section ratio may increase, and thus direct ionization of the carbon atom is more likely, leading to the formation of $C^{3+}$ without charge transfer. Alternatively, for iodine charge state $q \geqslant 4$, resonant photoexcitation becomes possible, via 4d $\rightarrow$ (np), nf transitions [20, 21]. This can lead to the production of excited iodine ions, $I^{q+*}$, for instance by spectator Auger decays. In this case, charge transfer mechanism may occur if the ionic iodine internal energy is enough to ionize $C^{2+}$. Such a condition is energetically favourable for $q \geqslant 4$. In our simulation, we artificially ionize $C^{2+}$ just after the first charge transfer and find an excellent agreement with the KER mean value, as shown for the $C^{3+}$ channels by the thin dotted line in figure 3(c). This result supports the idea that $C^{3+}$ channels are open at the same time as the $C^{2+}$ channels due to the ionization dynamics in the 4d-shell.

To gain some insights into the charge delocalization in the methyl group before production of $C^{3+}$ ions, we investigated the angle between the direction of the hydrogen ejection and the molecular axis (given by the $C^{p+}$–$I^{q+}$ momentum correlation, with $p = 1, 2$). This hydrogen emission angle can be experimentally retrieved from correlated momenta between $C^{p+}$–$I^{q+}$–$H^+$ momenta in a small subset of data with triple coincidence. We found that the experimental angle slowly decreases as function of the charge of iodine increases, as shown in figure 5(a). To reproduce this observation with our simulation, the assumption that all hydrogens are charged at the end of the fragmentation needs to be relaxed, and the initial neutral geometry of the molecule needs to be changed. Hence, by optimising these quantities and comparing the measured angles, the momentum correlation factor, the KER and branching ratios to the experimental data, an overall good agreement can be achieved, see figure 5(a). Our results suggest that the structure of the molecule has changed before the dissociation dynamic is governed by a Coulomb explosion as described by Vager *et al* [7] It is worth noticing that the measured angles slightly differ from the initial angles of the neutral molecule with values that are 3–7° higher due to the repulsion between atoms. Interestingly, in our simulation, the final effective charges of hydrogens is changing over the charge states of iodine, see figure 5(b). Though care should be taken in interpreting the simulation, the results provide an intuitive picture. Hydrogen atoms are progressively ripped from their charge as the iodine is ionized, and bare protons (with unit effective charge) are emitted at lower charge states of iodine for $C^{2+}$ channels than for $C^+$ channels.

## 5. Conclusion

We studied the sequential XUV multiphoton ionization of the I–4d shell in methyl iodide using coincidence and 3D momentum imaging spectroscopy. To understand the interplay between the fundamental processes leading to the charging of the molecule and the transfer of charges, we performed classical simulations of the Coulomb explosion by phenomenologically introducing ionization dynamics and charge transfers.

Within the COB model, the overall very good agreement between simulation and experiments indicates that the model provides a proper description of the ultrafast dynamics of the dominant fragmentation channels leading to the production of $C^+$ and $C^{2+}$ ions. For our experimental conditions, the photon absorption rate is below the Auger decay rate of ionic iodine, and tuning the Auger decay rate in our simulations is essential to predict the branching ratios. While the COB model is sufficient to describe our observation for the dominant fragmentation channels, a more complex interplay between ionization dynamics and charge transfer for the weakest fragmentation

channels with $C^{3+}$ ions is found. It is still possible to simulate the experimental results, but further investigations should be done.

Our results also point out that in some regime of light–matter interaction, a key factor for the fragmentation dynamics is the ratio between the dissociation speed and the charging rate. This ratio determines the number of charges accumulated before the charge transfer is forbidden. Since the speed of the dissociation dynamics can be controlled through ultra-fast dissociation [30, 31], it is possible to speed up (or slow down) nuclear motion (by changing the mass ratio between heavy and light elements). A prime interest for future studies is to investigate which of the ionization processes, carbon ionization or resonant Auger decay, primarily leads to the production of triply charged carbon ions. Such a study may also reveal the role of the chemical environment due to the methyl group at short internuclear distance.

## Acknowledgments

This work was supported by the European Union's Horizon 2020 research and innovation program under the Marie Skłodowska-Curie Grant Agreement No 641789 and No. 701647. PJ, SM and JL acknowledge support by the Swedish Research Council and Swedish Foundation for Strategic Research; D.Rol. and AR by the Chemical Sciences, Geosciences, and Biosciences Division, Office of Basic Energy Sciences, Office of Science, US Department of Energy, Grant No DE-FG02-86ER13491; DR, CB, and BE were also partially supported by the Helmholtz Gemeinschaft through the Helmholtz Young Investigator Program. We acknowledge the Max Planck Society for funding the development and the initial operation of the CAMP end-station within the Max Planck Advanced Study Group at CFEL and for providing this equipment for CAMP@FLASH. The installation of CAMP@FLASH was partially funded by the BMBF Grants 05K10KT2, 05K13KT2, 05K16KT3 and 05K10KTB from FSP-302. We would like to thank the scientific and technical team of FLASH for maintaining the facility and providing support during the beam time.

## Appendix A. Simulation

In our classical simulation, molecular dissociation proceeds during charging (through photoionization and Auger decay) and charge transfer [32]. The equation of motions are solved assuming point charges. The timing sequence of the ionization is given by a random number generator, weighted by the temporal distribution of the FEL intensity profile, which is assumed to be a Gaussian distribution. The ionization cross section of different iodine charge states are assumed to be the identical, which is justified for the first three ionization cross sections of ionic iodine [20, 21]. In figure 6, we present the average time between photon absorption events depends on the XUV pulse duration and the number of absorbed photons, shown as the blue region. Given the estimate of our experimental pulse width (purple region, assumed to be 40% ∼ 66% of

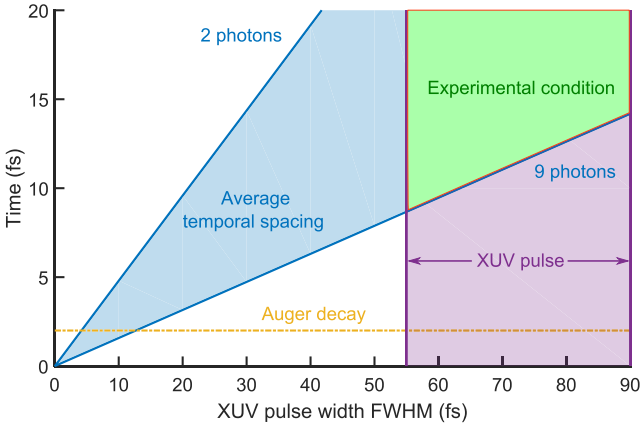


**Figure 6.** Estimated time scales as a function of XUV pulse width: the typical Auger decay time of neutral iodine (2 fs) is shown as a yellow dash-dotted line. The blue lines form the boundary for the average time interval between photon absorption, ranging from 2 to 9 photons (light blue area). The purple area represents the estimated XUV pulse duration, and the green intersection area represents our experimental range.

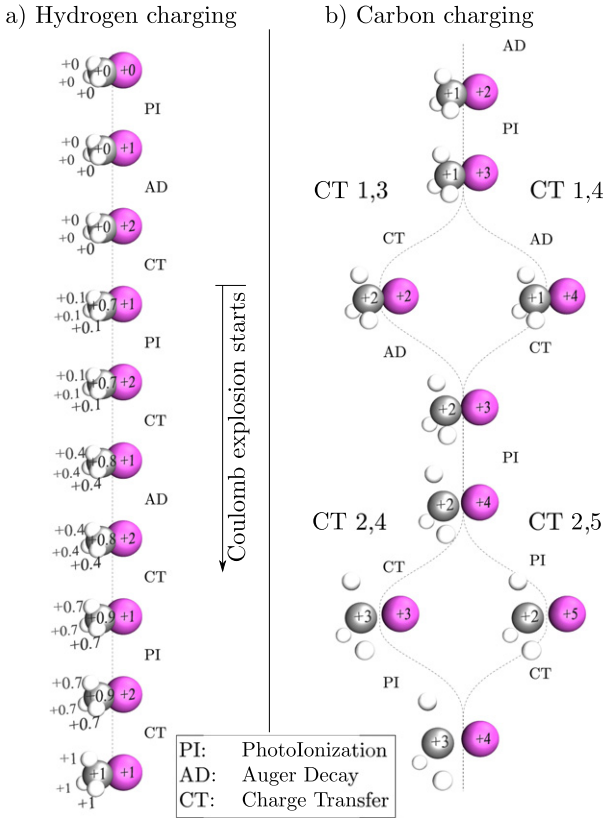


**Figure 7.** Charging mechanism of methyl iodide. (a) Initial charge depletion of hydrogen atoms, leading to proton ejection (b) followed by the charge transfer of carbon.

the electron bunch duration [23]), the Auger decay time (yellow dash-dotted line) is several times shorter than the average temporal spacing of absorption events.

In the model, the charging process is described as a sequence of photoionization and Auger decay events that occur separated in time. To determine the charging sequences,

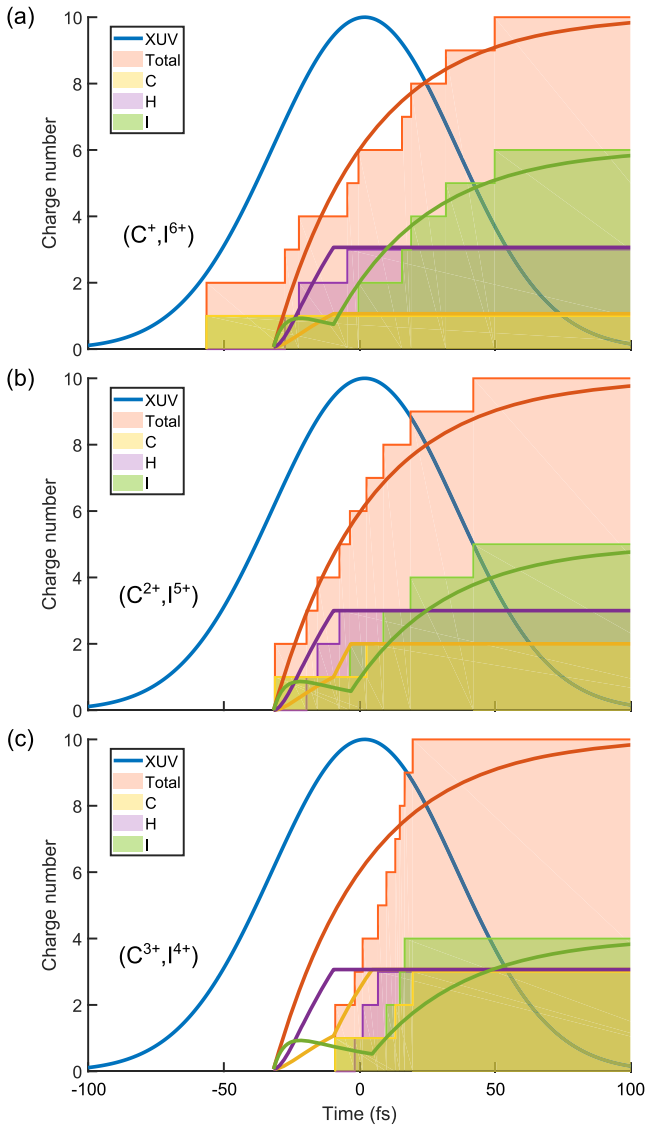


**Figure 8.** Time evolution of three different charge states with the same total number of charge for (a) $C^+$ channels, (b) $C^{2+}$ channels, and (c) $C^{3+}$ channels. The shaded areas are from our simulation, and the solid lines are the results from Motomura's model. The intensity profile of the (Gaussian) XUV pulse is indicated in blue.

we simulated first a two-body (carbon–iodine) break-up for charge states ($q \geqslant 3$) and determined the inter-nuclear distances and relative velocities for $C^+$–$I^{3+}$ and $C^+$–$I^{4+}$ that provide the best agreement for both kinetic energy released and branching ratios with our experimental results before and after charge transfer. In a second step, the full three-body break-up (in $C_{3v}$ geometry) was considered as a function of the initial fraction of charge in the methyl group, assuming complete ionization of hydrogen at the end. Practically, the initial fractional charge allows us to control the strength of the Coulomb force between the methyl group and iodine, i.e. the speed of dissociation. To best match the inter-nuclear distances and relative velocities found in the first step, as well as the experimental momentum correlation coefficient, hydrogen atoms have to act as an electron donor for the methyl group with a small initial fraction of charge (10%). Various charging sequences from the dominant ions produced after one photon absorption, $CH_3I^{2+}$ and $CH_3I^{3+}$, were then investigated. An overview of the entire charging process in our model is shown in figure 7. Initially, when neutral iodine absorbs a photon, it creates a doubly and a triply charged iodine atom with Auger and cascade Auger decay, followed by instantaneous charge redistribution, as shown in figure 7(a). After absorption of two or three photons, all three hydrogen atoms are fully charged. The fragmentation is then driven by the interaction between carbon and iodine atoms, and proceed with a sequence of charging and charge transfer steps, as shown in figure 7(b).

Finally, a complete optimization scan of all parameters (initial inter-nuclear distances and bond angle, pulse duration and fraction of charge) was performed, and the overall charging mechanism in time is compared to Motomura's model [16] in figure 8. In our model, the charging mechanism is progressively delayed within the envelop of the light pulse, reflecting the inherent time that it is taken to produce multiple charges. By adjusting the onset of the charging mechanism at −31.1 fs in Motomura's model with respect to the center of the light pulse, we found a good agreement between the two models for the $C^+$ and $C^{2+}$ channels. Our simulations suggest that the high charge states of the carbon have a faster charging mechanism and their production is temporally confined to the maximum of the FEL intensity, while in Motomura's model, the overall dynamics can extend over a much longer time scale.

## ORCID iDs

Yu-Chen Cheng https://orcid.org/0000-0002-7820-2935
Jan Lahl https://orcid.org/0000-0001-8563-0818
Sylvain Maclot https://orcid.org/0000-0001-5587-7182
Sven Augustin https://orcid.org/0000-0003-1283-331X
Severin Meister https://orcid.org/0000-0002-5245-8377
Dimitrios Rompotis https://orcid.org/0000-0002-2305-092X
Bastian Manschwetus https://orcid.org/0000-0001-6165-9560
Benjamin Erk https://orcid.org/0000-0001-8413-3588
Daniel Rolles https://orcid.org/0000-0002-3965-3477
Rebecca Boll https://orcid.org/0000-0001-6286-4064
Pavel Olshin https://orcid.org/0000-0002-0107-3258
Mathieu Gisselbrecht https://orcid.org/0000-0003-0257-7607

## References

[1] Ackermann W *et al* 2007 *Nat. Photon.* **1** 336
[2] Emma P *et al* 2010 *Nat. Photon.* **4** 641
[3] Allaria E *et al* 2012 *Nat. Photon.* **6** 699
[4] Ishikawa T *et al* 2012 *Nat. Photon.* **6** 540
[5] Young L *et al* 2010 *Nature* **466** 56
[6] Rudenko A *et al* 2017 *Nature* **546** 129
[7] Vager Z, Naaman R and Kanter E P 1989 *Science* **244** 426
[8] Fang L *et al* 2012 *Phys. Rev. Lett.* **109** 263001
[9] Braußе F *et al* 2018 *Phys. Rev.* A **97** 043429
[10] Amini K *et al* 2018 *Struct. Dyn.* **5** 014301
[11] Berrah N *et al* 2019 *Nat. Phys.* **15** 1279
[12] Erk B *et al* 2014 *Science* **345** 288

[13] Schnorr K *et al* 2014 *Phys. Rev. Lett.* **113** 073001
[14] Boll R *et al* 2016 *Struct. Dyn.* **3** 043207
[15] Fukuzawa H *et al* 2013 *Phys. Rev. Lett.* **110** 173005
[16] Motomura K *et al* 2015 *J. Phys. Chem. Lett.* **6** 2944
[17] Ryufuku H, Sasaki K and Watanabe T 1980 *Phys. Rev.* A **21** 745
[18] Niehaus A 1986 *J. Phys. B: At. Mol. Phys.* **19** 2925
[19] Mertens K, Gerken N, Klumpp S, Braune M and Martins M 2016 *J. Mod. Opt.* **63** 383
[20] Kjeldsen H, Andersen P, Folkmann F, Knudsen H, Kristensen B, West J and Andersen T 2000 *Phys. Rev.* A **62** 020702
[21] Domondon A and Tong X 2002 *Phys. Rev.* A **65** 032718
[22] Erk B *et al* 2018 *J. Synchrotron Radiat.* **25** 1529–40
[23] Duesterer S *et al* 2014 *Phys. Rev. Accel. Beams* **17** 120702
[24] Schnorr K 2014 *XUV Pump–Probe Experiments on Diatomic Molecules* (*Tracing the Dynamics of Electron Rearrangement and Interatomic Coulombic Decay*) (Berlin: Springer)
[25] Manura D and Dahl D SIMION (R) 8.1 User Manual (Adaptas Solutions, LLC) Palmer, MA 01069 http://simion.com/ (Accessed: January 2008)
[26] Erk B *et al* 2013 *Phys. Rev. Lett.* **110** 053003
[27] Cutler J N, Bancroft G M and Tan K H 1992 *J. Chem. Phys.* **97** 7932
[28] Bizau J, Blancard C, Cubaynes D, Folkmann F, Champeaux J, Lemaire J and Wuilleumier F 2006 *Phys. Rev.* A **73** 022718
[29] Watanabe N *et al* 1998 *J. Phys. B: At. Mol. Opt. Phys.* **31** 4137
[30] Travnikova O, Kimberg V, Flammini R, Liu X-J, Patanen M, Nicolas C, Svensson S and Miron C 2013 *J. Phys. Chem. Lett.* **4** 2361
[31] Morin P and Miron C 2012 *J. Electron Spectrosc. Relat. Phenom.* **185** 259
[32] Cheng Y-C 2019 Ultrafast photoionization dynamics studied with coincidence momentum imaging spectrometers *PhD Thesis* Lund University